INTERNATIONAL JOURNAL OF INTEGRATED ENGINEERING
ISSN: 2229-838X e-ISSN: 2600-7916

IJIE

Vol. 16 No. 6 (2024) 265-284
https://publisher.uthm.edu.my/ojs/index.php/ijie

A Comprehensive Review of Modeling Approaches for Analyzing Mechanical Properties and Fatigue Performance in Magnesium Alloys

Raj Kumar[1]*, Mohammad Mursaleen[1], G. A. Harmain[1]

[1] *Mechanical Engineering Department,*
National Institute of Technology Srinagar, Hazratbal, Srinagar, Kashmir - 190006, INDIA

*Corresponding Author: raj19_phd@nitsri.ac.in
DOI: https://doi.org/10.30880/ijie.2024.16.06.026

Article Info

Received: 20 August 2024
Accepted: 24 November 2024
Available online: 29 December 2024

Keywords

Magnesium alloy, fatigue, mechanical properties, load ratio

Abstract

Abstract magnesium (Mg) alloys have garnered considerable attention across diverse sectors, encompassing aerospace, automotive, and biomedical domains, owing to their advantageous attributes, which include a notably low density (1.7 g/m^3), high strength-to-weight ratio, augmented specific stiffness, heightened damping capacity, and exceptional machinability. This paper provides a comprehensive review of the influence of strain amplitude, strain rate, and temperature on the fatigue life of magnesium alloys. The investigation entails a comparative analysis of fatigue life modeling using established models such as Walker's and Wheeler's models, employing a synthesis of experimental and analytical methodologies. Furthermore, the monotonic mechanical properties, encompassing tensile strength and yield stress, are elucidated across a wide temperature range from room temperature (RT) to 300°C, alongside a comparative evaluation vis-a-vis other material counterpart. The paper also encapsulates a comprehensive review and tabulation of the limited analytical studies pertaining to magnesium alloys available in the literature.

1. Introduction

Magnesium (Mg) alloys are potential candidates for use as structural materials in the automobile, aviation industries and electronic sectors [1–5]. Magnesium alloys have caught the attention of designers because of their relatively lower density, higher strength-to-weight ratio, better specific stiffness, improved damping capacity, superior machinability, good electromagnetic shielding, and ease to recycle [5–14]. In recent past, the investigation into lightweight structures has been focussed on magnesium alloys owing to their exceptional specific strength and ease of machining [15]. For automobile applications, magnesium alloys are being sought as a replacement for steel and aluminium alloys due to possible improvements in fuel economy and reduced emissions. In automobiles, these components may be found in the following places: engine blocks, transfer cases, and transmissions [16].

The possibility of replacement of steel and aluminium alloys in some applications with magnesium alloys. Magnesium alloys are the least heavy metals that are used for structural purposes. Compared to aluminium alloys, these are 33% lighter, and 75% lighter than steel [17,18]. The outstanding toughness-to-weight ratio of Mg alloys allows for lighter armoured vehicles to be used today [19]. Mg alloys are recognised as better materials with reduced energy consumption and relatively less contamination of the environment [20], so their usage has increased in modern years [21,22]. It's important to look at the fatigue properties of Mg alloys for their possible utilize in load-bearing parts (such as engine and transmission parts) under tough conditions

This is an open access article under the CC BY-NC-SA 4.0 license.

including high temperatures. The evaluation of Mg alloy's ability to withstand cyclic loading is heavily dependent on analyzing the fatigue crack propagation (FCP) behavior [23].

Casting processes are commonly employed in the production of a variety of Mg alloy items; however, their application in large-scale construction remains somewhat restricted [24]. Wrought Mg alloys demonstrate improved mechanical properties such as higher tensile strength and fatigue resistance when compared to cast Mg alloys [25,26]. The limited availability of slip systems in Mg alloys results in considerable differences between tension and compression behaviors (T-C asymmetry) and noticeable variations in plastic deformation anisotropy [27]. The magnesium alloy, when subjected to monotonic loading may result in plastic deformation and twining accompanied by a hardening phenomenon before fracture. As the plastic deformation starts with a slip under monotonic loading, there may be different degrees of hardening. However, when the material is further strained, the softening rates have a tendency to become more uniform [15].

Extruded AZ31B magnesium alloys have exhibited superior performance when contrasted with cast Mg alloys. The luggage shelves of the bullet trains are made up of AZ31B magnesium alloys and it has been seen that the weight of luggage shelves is reduced by 33% by using AZ31B alloy. The strength and toughness of AZ31B Mg alloy are 1.25 and two times that of 6063 Al alloy respectively. It has been demonstrated that employing AZ31B Magnesium alloy is an effective approach for achieving energy savings and ensuring protection and safety control [28]. According to Roodposhti et al. [29], the brittle fracture morphology of AZ31 Mg alloy at 623K was mostly caused by quick grain development under high temperature and low stress, which led to grain boundary sliding creep deformation. However, as the stress and strain rates increased, a ductile fracture appeared, which consisted of numerous small dimples and tearing edges.

Rodriguez et al. [30] informed that the tensile strain to fracture (ε_f) of cast magnesium alloy AZ31B increases with rising temperature and decreases with decreasing strain rate. Under various deformation conditions, several other Mg alloys, such as Mg alloy AZ31 [31,32] and AM30 Mg alloy [33,34], have exhibited a similar tendency near fracture. Zeng et al. [35] reported that the reduction in loading frequency resulted in an rise in FCG rate in an extruded magnesium alloy. Furthermore, research has indicated that the FCG rate of Mg alloys, like other metals, rises with load ratio (R) [36–38]. Although extensive research has been performed on the fatigue characteristics of these Mg alloys at RT, our understanding of their low-cycle fatigue (LCF) behavior at elevated temperatures remains limited. Moreover, there isn't much research done on fracture behaviour of Mg alloys, particularly under the different overload ratios (OLR) that are typical in the aerospace and automotive sectors. This paper aims to provide a summary of the mechanical characteristics of magnesium alloys subjected to both monotonic tension and compression, as well as an exploration of their fatigue behavior through various models.

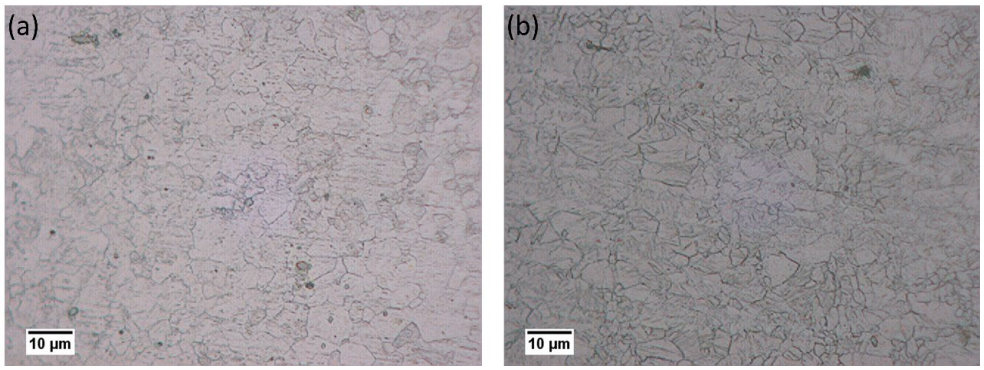

Fig. 1 *(a) and (b) displays a microstructure of AZ31B Mg alloy*

2. Experimental Studies

2.1 Microstructure

The microstructure of Mg alloys has a substantial impact on their mechanical properties. A decrease in processing temperature and an increase in extrusion ratio lead to a decrease in the grain size of AZ31B Mg alloys [39]. The fatigue strength is improved by grain size refining. Typically, when grain size decreases, the twinning stress increases [40]. Tensile strength increased and crack growth resistance decreased with increasing precipitate density [35,41]. It has been observed that wrought magnesium alloys featuring an uneven microstructure exhibit a reduced rate of fatigue crack growth (FCG). Crack branching causes a deviation in the trajectory of the primary crack propagation (CP), occurring along the plane characterized by the highest normal stress [36–38]. Fig. 1(a) and 1(b) displays a cross-sectional microstructure of the Mg alloy AZ31B. The material

Int. Journal of Integrated Engineering Vol. 16 No. 6 (2024) p. 265-284

exhibited a bimodal distribution of grain sizes, comprising both very small and large grains. The cross-section has a grain size of about 20 μm on average. According to energy dispersive spectroscopy (EDS) analyses, the black spots on the photos were manganese (Mn) and aluminium (Al) containing elements [8]. The chemical composition of different magnesium alloys is presented in Table 1, while Table 2 illustrates the microstructural characteristics and grain size of different magnesium alloys. Table 2 summarizes numerous investigations showed on the effect of grain size on the mechanical properties of Mg alloys. Meanwhile, Tables 3 and 4 examine the application and advantages of Mg alloys respectively.

Table 1 *Different Mg alloys chemical compositions (in weight %)*

Author	Material	Al	Zn	Mn	Ca	Cu	Fe	Ni	Si	Zr	Y	Mg
Ishihara et al. 2009 [1]	AZ31	3.10	0.79	0.35	-	0.0023	0.0041	0.0008	0.019	-	-	Balance
Zheng et al. 2013 [5]	AZ31B	2.5-3.5	0.7-1.3	0.2	-	0.05	0.005	-	0.3	-	-	Balance
Yu et al. 2017 [11]	AZ31B	3.28	1.0	0.44	-	0.00039	0.0029	0.00023	0.025	-	-	Balance
Anes et al. 2021 [18]	AZ31B-F	3.1	1.05	0.54	0.04	0.0008	0.0035	0.0007	0.1	-	-	Balance
Luo et al. 2010 [20]	AM30	3.4	0.16	0.33	-	0.0008	0.0026	0.0006	-	-	-	Balance
Nan et al. 2007 [22]	AZ31	2.5-3.5	0.7-1.3	0.2	0.04		0.005	0.005	0.05			Balance
Xu et al. 2007 [23]	Mg-Zn-Y-Zr	-	6.26	-	-	-	-	-	-	0.78	0.66	Balance
Chen et al. 2007 [25]	AM50	4.4-5.4	0.22	0.26-0.6	-	0.01	0.004	0.002	0.1	-	-	Balance
Uematsu et al. 2009 [39]	AZ61	6.76	0.74	0.22	-	0.004	0.002	<0.001	0.043	-	-	Balance
	AZ80	8.4	0.6	0.3	-	0.003	0.003	<0.001	0.03	-	-	Balance
Zeng et al. 2009 [41]	AM60	5.60-6.40		0.26-0.50	-	≤0.008	≤0.004	≤0.001	≤0.05	-	-	Balance
Wu et al. 2008 [42]	ZK60A	-	6.0	-	-	-	-	-	-	0.5	-	Balance
Horstemeyer et al. 2004 [43]	AZ91E-T4	8.1-9.3	0.40-1.0	0.17-0.35	-	0.015	0.005	0.001	0.20	-	-	Balance
Eisenmeier et al. 2001 [44]	AZ91	9.0	1.0	0.5	-	-	-	-	-	-	-	Balance
Rozali et al. 2009 [45]	AZ61	5.95	0.26	0.0007	-	0.009	0.64	0.005	0.0008	-	-	Balance
Feng et al. 2014 [46]	AZ31B	3.19	0.81	0.334	-	0.005	0.005	-	0.02	-	-	Balance
Albinmousa et al. 2011 [47]	AZ31B	3.10	1.05	0.54	-	0.0008	0.0035	0.0007	-	-	-	Balance

2.1.1 Tensile and Compressive Properties

The monotonic tension and compression specimen orientation of several Mg alloys are illustrated in Fig. 2. Monotonic tension and compression stress vs strain curves are correlated for different Mg alloys, along with, AZ31 [1,7], AZ31B [14,70,85], AM30 [33], AM60 [41], AZ41 [66] and ZK60 [81] are depicted in Fig. 3 (a & b). The monotonic behaviour of AM30 [33,63], AM60 [41], ZK60 [81], AZ31 [1,86], and AZ31B [87,88] seems to be of a power-law nature when the tensile curves for extrusion direction (ED) are considered (Fig. 3(a)). Fig. 3(b) compares the compressive stress vs strain curves of the AZ31 [1,86], AZ31B [14,89], TAZ811 [24], and ZK60 [81]. From this Figure, it is evident that when alloys are loaded along the ED, their behaviour after yielding is concave. A typical explanation for this peculiar behaviour is that the twinning deformation is initiated as a result of the loading orientation to the texture. In Fig. 4(a) and 4(b), monotonic tensile and compressive characteristics

for the magnesium alloys AZ31 [7], AZ31B [85,89], AM30 [33], and AZ41 [66] rolling at various orientations are compared. Two graphs with stress-strain curves were drawn to illustrate the differences. According to Fig. 4(a), the tensile curves exhibit power-law behaviour after yielding. The compressive curves in Fig. 4(b) exhibit a sigmoidal-shaped pattern with concave upward characteristics. However, Fig. 4(a) and 4(b) demonstrate that there are distinct variations in the tensile and compressive properties between the normal and transverse orientations.

Table 2 *Microstructural details and grain size for various Mg alloys*

Author	Material	Direction	Size (μm)	Structure	Remarks	Intermetallic compound
Nan et al. 2007 [22]	AZ31	ED	22.5	Circular region	Light layer (region A), the dark layer (region B)	$Mg_{17}Al_{12}$
Park et al. 2010 [24]	TAZ811	ED	100-400	Fine-grain	Compared to AZ31, TAZ811 exhibits a significantly smaller grain size.	Mg_2Sn
	AZ31	ED	200			Al-Mn Particles
Chen at al. 2007 [25]	AM50	ED	15	Lamellar precipitates	Fine and equiaxed $\alpha - Mg$ grains	$\beta - Mg_{17}Al_{12}$
Uematsu et al. 2009 [39]	AZ61	ED	13	Lamellar like-precipitates	The boundary between the inclusion and the matrix, or the separation of the inclusion.	$Mg_{17}Al_{12}$
	AZ80	ED	13			
Zeng et al. 2010 [41]	AM60	ED	56	Square	-	$Mg_{17}Al_{12}$
		ED	17			
Xu et al. 2009 [33]	AM30	ED	32	-	Twins are observed	-
Tokaji et al. 2009 [48]	AZ31	ED	60	Equiaxed grain structure	Crystallographic texture	-
	AZ61	ED	14			
Horstemeyer et al. 2004 [43]	AZ91E-T4	ED	S1-105 S2-110 S3-140	Granular and dendritic structure	Dendritic structure within the grains.	$\beta - Mg_{17}Al_{12}$
Rozali et al. 2009 [45]	AZ61	ED	15	-	A large number of slips occur in some grains	-
Albinmousa et al. 2011 [47]	AZ31B	ED	7.4	-	Finer grain at the core	-

Table 3 *Uses of magnesium alloys*

Military and aerospace	Automobile	User products
Aircraft air frames[49]	Engine blocks[2][16][38]	Portable computers[2][50]
Engines[51]	Transfer cases[16][38]	Cell phones [52]
Cockpit Instrument Panel and Service Door Inner Panel [53]	Gear boxes[16][38][53]	Cameras [50]
Electronic housing [54]	Brackets and Panels [16][38]	
Missile skins and frames [54]	Car body[51]	
Transmission cases[51]	Wheel, steering columns, seat frames, fuel tanks [53], Auto steering wheel frame [55], [56], rocker rails [83], and Valve covers [57].	
Tail gearbox (TGB) housing [58]		

Table 4 *The advantages of Mg alloys*

Properties	Advantages	References

Int. Journal of Integrated Engineering Vol. 16 No. 6 (2024) p. 265-284

Specific strength	Mg has a specific strength comparable to cast iron and equal to or higher than several conventional automotive aluminium alloys, which enables it to reduce bulk more effectively than aluminium.	[1][2] [3][5][6][15][51]
Specific stiffness	Magnesium is stiffer than many polymeric materials and composites, so it can be used to make things lighter.	[4] [7][51]
Damping capability	Magnesium alloys are good because they have better damping properties than other materials.	[1][2][9]
Low-temperature properties	Mg doesn't change from being hard to be soft, so it can be used at very low temperatures.	[59]
Machining	Magnesium outperforms aluminium in terms of tool durability and cost. The main problem is the extra caution needed while handling machining chips.	[5][6][8] [5][15]
Fluidity	Because magnesium has high fluidity, it can be cast into shapes with walls as thin as 1.5 mm. This makes it easier to reduce mass.	[28]
Hot formability	Utilizing high-temperature forming techniques, wrought magnesium may be shaped into exceedingly intricate forms.	[14][26][60][61][31]

2.2 Monotonic Behavior

The stress vs strain curves for different alloys, including AZ31 [7], AZ31B [1,2], AZ61 [45,48], AZ91 [62], AM30 [33,63] and AM60 [41] are compared for both monotonic tension and compression in Table 5 and 6.

Table 5 *Monotonic tensile properties of different Mg alloys*

Author	Material	Direction	Modulus of elasticity (E) (GPa)	Yield stress ($\sigma_{y,0.2\%}$) (MPa)	Ultimate tensile stress (σ_u)(MPa)	% Elongation
Ishihara et al. 2009 [1]	AZ31B	ED	45.0	206	282	21.8
Hongxia et al. 2011 [2]	AZ31B	ED	-	110-150	220-250	7-8
Han et al. 2014 [7]	AZ31	ED	-	180	260	-
		TD		80	230	-
Jabbari et al. 2020 [14]	AZ31B	ED	45.2	245	322.3	8.9
Ishihara et al. 2007 [21]	AZ31	ED	45	200	275	11
Nan et al. 2007 [22]	AZ31	ED	45	200	275	11
Park et al. 2010 [24]	TAZ811	ED	-	245	310	18.5
	AZ31	ED	-	180	268	23.5
Chen et al. 2007 [25]	AM50	ED		260	300	14
Zeng et al. 2010 [41]	AM60	ED	-	186	266	22.0
Begum et al. 2009 [64]	AZ31	ED	45	201	264	15.2
Xu et al. 2009 [33]	AM30	ED	-	196	250	12.3
		TD	-	76	239	19.1
Tokaji et al. 2009 [48]	AZ31	ED	-	110	224	30
	AZ61	ED	-	-	278	25
Yang et al. 2008 [51]	AZ31	ED	-	187.2	294.5	18.5
Rozali et al. 2009 [45]	AZ61	ED	43	200	290	18
Park et al. 2010 [65]	AZ31	ED	-	153	281	12.4
		ND	-	53	330	14.5
Prakash et al. 2020 [66]	AZ41	ED	-	177	219	13.5
Anes et al. 2016 [67]	AZ31B-F	ED	45	211	290	14
Zhou et al. 2016 [68]	AZ31B	ED	-	182	227	15.3
		DD	-	69	218	20.1
		TD	-	64	237	15.8
Albinmousa et al. 2010 [63]	AM30	ED	43.99	164.06	244.41	14.89

Gryguc et al. 2019 [69]	AZ80	ED	46.8	197.3	341.1	11.3
		Forged	44.7	286.0	384.9	15.3
Xiong et al. 2012 [70]	AZ31B	ED	44.8	244	298	10.5
Albinmousa et al. 2011 [71]	AZ31B	ED	43.72	213.33	227.45	10.01
		45°	43.5	65.67	208.95	17.51
		TD	40.59	55.67	246.62	9.38
Hasegawa et al. 2007 [72]	AZ31	ED	45	205	252	17.3
Khan et al. 2009 [73]	WE43		-	180	265	7
	Elektron 21		-	175	265	7
Begum et al. 2009 [74]	AZ31	ED	-	201	264	15.2
Mirza et al. 2014 [75]	NZ30K	ED	-	180	225	9.1
	GW103K	ED	-	232	318	8.3
Ni et al. 2014 [62]	AZ91D	ED	-	192	245	7.6
Nascimento et al. 2010 [76]	AZ31	ED	-	197	269	19
	ZN11	ED	-	108	210	39
He et al. 2017 [77]	ZK60	ED	45	286.3	348.5	11
Albinmousa et al. 2020 [78]	ZK60-T5	ED	44.29	220.7	284.0	17.65
G. Junak 2020 [79]	WE43	ED	42.8	224.2	311.1	16.5
	AZ31	ED	43.7	225.2	316.5	16.6
Q. Yang and A.K. Ghosh 2006 [80]	AZ31B	ED	-	160	274	13.5
Yu et al. 2012 [81]	ZK60	ED	45	279	364	16.7

Table 6 *Monotonic compressive characteristics for various Mg alloys*

Author	Material	Direction	Yield stress ($\sigma_{y,0.2\%}$) (MPa)	Ultimate compressive strength (σ_{UCS}) (MPa)	Deformation (%)
Ishihara et al. 2009 [1]	AZ31B	ED	123	276	11.6
Jabbari et al. 2020 [14]	AZ31B	ED	166.4	306.3	15.0
Park et al. [82]	AZ31	ND	128	273	18.5
		RD	66	292	17.5
Albinmousa et al. 2011 [47]	AZ31B	ED	108	364.1	12.6
		45°	94	230.3	16.8
		TD	127	316.7	5.3
Gryguc et al. 2019 [69]	AZ80	ED	155.5	341.1	11.3
		RD	116.4	290.2	15.3
		Forged	161.8	384.9	15.3
Xiong et al. 2012 [70]	AZ31B	ED	151	417	9.3
Nascimento et al. 2010 [76]	AZ31	ED	109	352	10
	ZN11	ED	100	323	16
Yu et al. 2012 [81]	ZK60	ED	171	190	5
Morita et al. 2010 [83]	AZ31B	ED	75	253	11.5
Mirza et al. 2013 [84]	Mg–10Gd–3Y–0.5Zr	ED	232	493	18.7
Wu et al. 2010 [85]	AZ31B-H24	ND	150	331.4	3.7
		RD	100	354.3	9.7
		TD	86	323.2	10

Int. Journal of Integrated Engineering Vol. 16 No. 6 (2024) p. 265-284

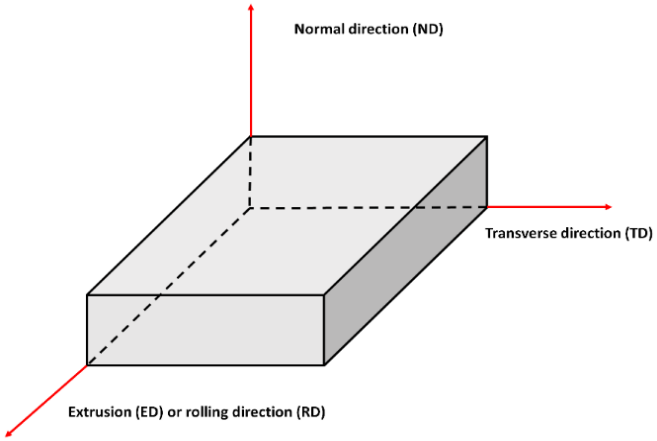

Fig. 2 *Description of material orientation*

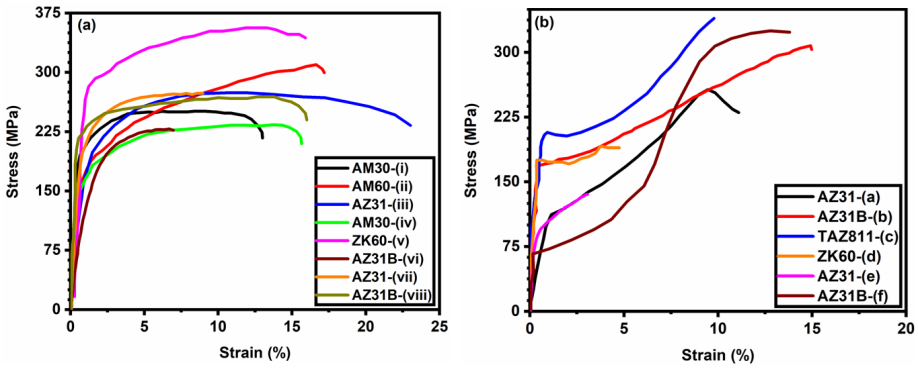

Fig. 3 *Monotonic stress versus strain curves for various Mg alloys at extrusion directions. (a) Tension; (b) Compression. In legend: (i) Xu et al., 2009, (ii) Zeng et al., 2010, (iii) Ishihara et al., 2009, (iv) Pascu et al., 2010, (v) Yu et al., 2011, (vi) Li et al., 2021, (vii) Lei et al., 2021, (viii) E. A. Pressing, 2021. (a) Ishihara et al., 2009; (b) Jabbari et al., 2020; (c) Park et al., 2010; (d) Yu et al., 2011; (e) Lei et al., 2021; (f) Qiao et al., 2021*

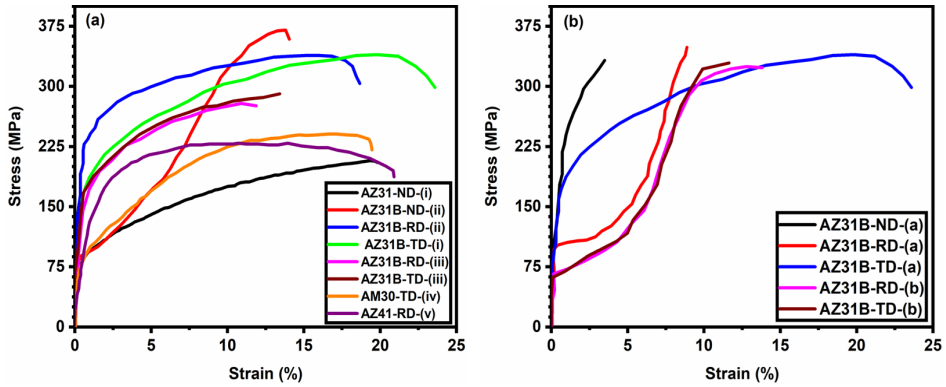

Fig.4 *Monotonic stress versus strain curves for various Mg alloys at different directions. (a) Tension; (b) Compression. In legend: (i) Han et al., 2014, (ii) Wu et al., 2010, (iii) Qiao et al., 2021, (iv) Xu et al., 2009, (v) Singh et al., 2020. (a) Wu et al., 2010; (b) Qiao et al., 2021*

2.3 Fatigue Behavior

2.3.1 Effect of Strain Amplitude

The stress softening rate increases as the applied strain amplitudes increase. Also, the samples that were subjected to high strain amplitudes under tensile loads softened more at the beginning and end of the test, which may be related to dynamic recrystallization (DRX) and damage [14]. Even at the smaller strain amplitudes, cyclic stability was only just attained. Mg alloy NZ30K showed cyclic softening and hardening with low strain amplitudes (0.2%) and high strain amplitudes (0.4% up to 1.0%), respectively. Fig. 5 illustrates the initial cyclic hardening observed during the initial three cycles, employing a higher strain amplitude of 1.2 percent, followed

by subsequent cyclic softening. However, it was noted that the fatigue life of this magnesium alloy was equivalent to that of other magnesium alloys [75]. During low-cycle fatigue (LCF) testing, it was observed that the WE43 alloy exhibited persistent cyclic hardening and partial cyclic softening at relatively low strain amplitudes. When subjected to higher strain amplitudes, the alloy rapidly undergoes initial hardening within a few cycles, followed by a subsequent minor softening leading up to failure [90]. The effect of the increased strain magnitude wasn't as noticeable as the effect of the decreased opening load caused by crack closure. This means that the crack closure has a prominent effect and lasts for more time than the plastic strain effect near the crack tip region [91].

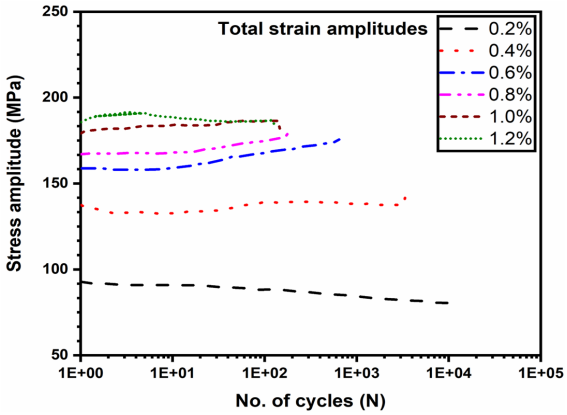

Fig. 5 *The stress amplitude vs No. of cycles (N) for the NZ30K alloy at various strain amplitudes with a strain ratio of R_ε = -1 [75]*

2.3.2 Effect of Strain Rate

Kim et al. [61] performed uniaxial tensile test to observed the mechanical properties and fracture strain (ε_f) of the AZ31 at a broad range of temperatures (323-523 K) and strain rates ($2x10^{-4}$ to $1x10^{-1}s^{-1}$). The correlation between fracture strain, temperature, and strain rate is depicted in Fig. 6. The depicted Figure demonstrates that raising the temperature and lowering the strain rate typically lead to an increase in fracture strain. The degree of plastic anisotropy increases as the strain rates increase within the range of (10^{-4} and 10^{-2} s^{-1}), except at 373K [30]. At all temperatures, normal direction compression curves exhibit the same shapes as in-plane tension curves in terms of yield and flow stresses, as demonstrated in [32]. The impact of temperature and strain rate on specimens oriented in the transverse direction (TD) is less pronounced in the early stages of deformation, primarily because of the heightened prevalence of twinning activity in these samples in contrast to those aligned with the extrusion direction [33]. The strain to failure decreases at higher strain rates and room temperature. However, an increase in strain rate leads to an increase in elongation at fracture in the AZ31B Mg alloy between 373K and 523K. At high temperatures, the flow stress decreases, but elongation at fracture increases significantly [46].

The AZ41 magnesium alloy is found to be more ductile and tough at lower strain rates (0.0001- 0.1 s^{-1}) then at higher strain rates (600-1150 s^{-1}) [66]. The improvement of fatigue life in AZ31 Mg alloy was attributed to a combination of factors including cyclic hardening rate, plastic strain, stress amplitudes, and mean stress. At high strain rates and low strain ratios or mean strains, the fatigue life of the AZ31 was notably enhanced due to the combined impact of cyclic hardening rate, plastic strain, stress amplitudes, and mean stress. The fatigue crack initiation (FCI) stage was observed to be faster, but the CP stage was significantly prolonged, resulting in an overall longer fatigue life at higher strain rates [74]. The experimental data obtained for (σ_u), (σ_y), and strain hardening exponent (n) were in agreement with the results reported by Jiang et al. [92]. The investigation revealed that within the low strain rate range of ($5.3x10^{-3}$ s^{-1} to $1.47x10^{-2}$ s^{-1}), there was an increase in both σ_u and σ_y while the *n* values declined with the rise of strain rate.

Int. Journal of Integrated Engineering Vol. 16 No. 6 (2024) p. 265-284

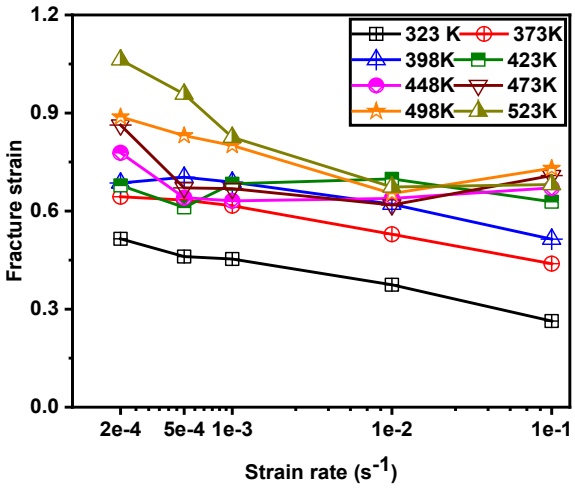

Fig. 6 *Fracture strain vs strain rate at various temperatures [61]*

2.3.3 Effect of Temperature

In an ambient temperature strain-controlled LCF experiment on Mg alloy AZ31 conducted by Chen et al. [64], it was observed that the ultimate compressive stress varied significantly with an rise in the strain range. This effect was ascribed to the antagonism between twinning-detwinning and dislocation slip processes. According to the authors, the plastic deformation at room temperature is significantly influenced by twinning-detwinning processes, which result in the creation of asymmetric hysteresis loops. When subjected to cyclic loading at ambient temperature, the mean stress can be determined, particularly at high strain amplitudes. Nevertheless, as the temperature rises, the mean stress decreases [14]. As the temperature increased, the material exhibited an increasing positive strain rate sensitivity (SRS) starting from the ambient temperature. The decreased strain rate was accompanied by an rise in the temperature sensitivity of the material [32]. Guo et al. [53] conducted stress-controlled cyclic loading experiments on a magnesium alloy across different temperatures within the LCF regime. The maximum and minimum cycle stresses were selected as proportions of the alloy's (σ_u) at room temperature. The findings demonstrated that stress concentration significantly influences the fatigue behavior of an alloy at RT. However, this sensitivity diminishes at elevated temperatures.

The study on cyclic deformation of Mg alloy AZ91 under strain-controlled conditions at varying temperatures revealed that the Coffin-Manson-Basquin (CMB) relationship can correlate total strain amplitude and fatigue life [44]. The material becomes more ductile at elevated temperatures, resulting in decreased fatigue damage under strain-controlled conditions throughout the loading cycle. Higher temperatures cause a material's strength to decrease and its plastic strain amplitude to increase. However, the samples' fatigue lifetimes are the same at a range of temperatures [14]. At temperatures below a critical point, the hardening behavior was noted to be distinct, and the degree of asymmetry during cyclic loading varied with temperature. Particularly, the stress-strain curves displayed distinct characteristics below the transition temperature, with a concave-up appearance during compression loading and an S-shaped appearance during tension loading after compression. Conversely, above the transition temperature, the flow curve adopted the conventional shape [93]. At 423K, cyclic loading along the direction of extrusion makes an asymmetric loop shape, even though the material has an asymmetric hysteresis loop at room temperature and low temperatures. There are also reports of twinning at high temperatures, though the number of twins is lower and it starts at higher stress levels, which suggests a slow activation. At RT and cryogenic temperatures, twining is the dominating deformation mechanism as shown in Fig. 7. At high temperatures, more slip planes are active and twinning activities are reduced, so the deformation mode is slip-dominated [60].

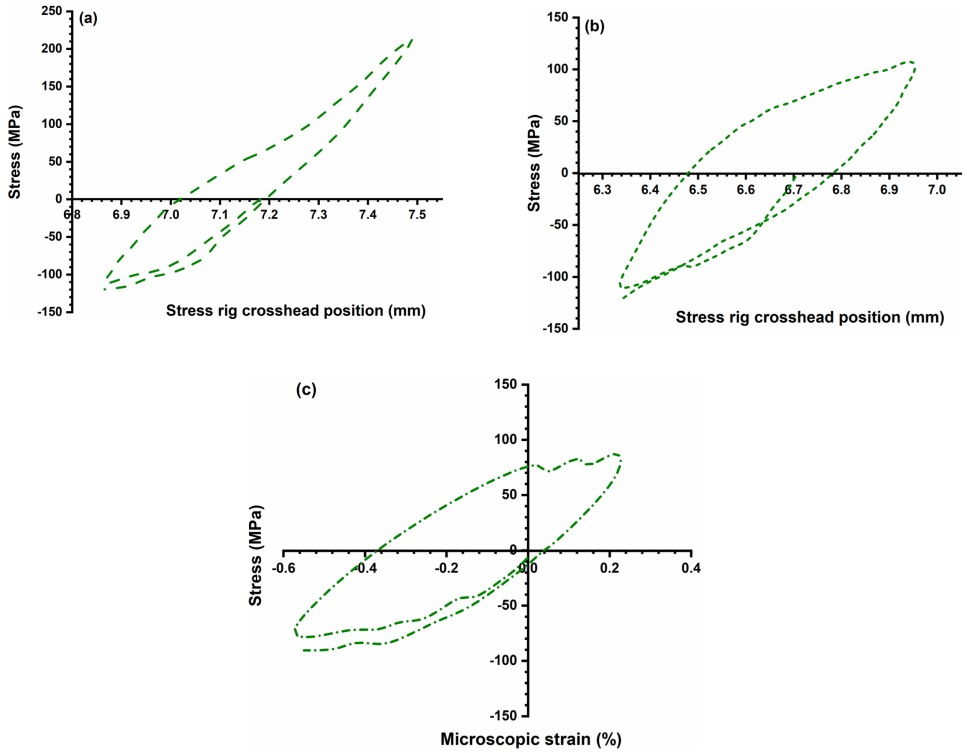

Fig. 7 *Macroscopic stress versus strain responses (a) extrusion direction (at -100°C); (b) transverse direction (at -100°C), (c) extrusion direction (at 150°C) [60]*

The deformation at high temperatures in AZE911 magnesium alloy revealed the existence of both basal and non-basal dislocations. The fatigue strength of the alloy experiences a substantial reduction at temperatures exceeding 473K, which could be attributed to the activation of slip structures other than the basal type. Hence, the AZE911 alloy experiences an escalation in dislocation cross-slip, which appears to be the primary cause for its softening at elevated temperatures [57]. Roodposhti et al. examined the fracture behavior of AZ31 after high-temperature tensile deformation under a constant load ranging from 1-13 MPa at 623K [29]. The study revealed that the longitudinal strain to failure (ε_f) increased with a rise in temperature and a decline in strain rate. When temperatures are high and strain rates are low, the tendency is very dominated [30]. Fig. 8 illustrates the hysteresis loops of engineering stress vs. strain for the initial and subsequent half-life cycles. These cycles illustrate total strain amplitudes of 0.2% and 1.0% and are presented for both the as-cast and forged AZ31B materials [94]. It is significant that the observed serrations, identifiable by stress drops and subsequent reloading to plateau stress, within the hysteresis loops during the compressive reversal phase in the circumstance of the forged material [94].

Low strain rates and higher temperatures caused the failure strains to become larger. Even though there was no twining after large deformation at higher temperatures, the orientation of the grains changed in a way that was similar to at room temperature. At elevated temperatures, the fracture surface displayed entirely ductile fracture characteristics, while at room temperature, it exhibited quasi-brittle fracture behavior [32]. When subjected to high strain rates, the AZ31B magnesium alloy sheet displays a significant softening effect above 423K. However, quasi-static tensile tests, which employ low strain rates, do not account for the adiabatic temperature rise effect. However, this effect is important in dynamic tension. At different temperatures, the adiabatic temperature will rise to different degrees when the strain rate is high. Under high strain rates, the adiabatic temperature increase has the potential to alter the material's microstructure and mechanical properties [46]. Raising the temperature from RT to a maximum of 473K leads to a reduction in flow stress and a concurrent enhancement in ductility for the AZ41 magnesium alloy [66].

Int. Journal of Integrated Engineering Vol. 16 No. 6 (2024) p. 265-284

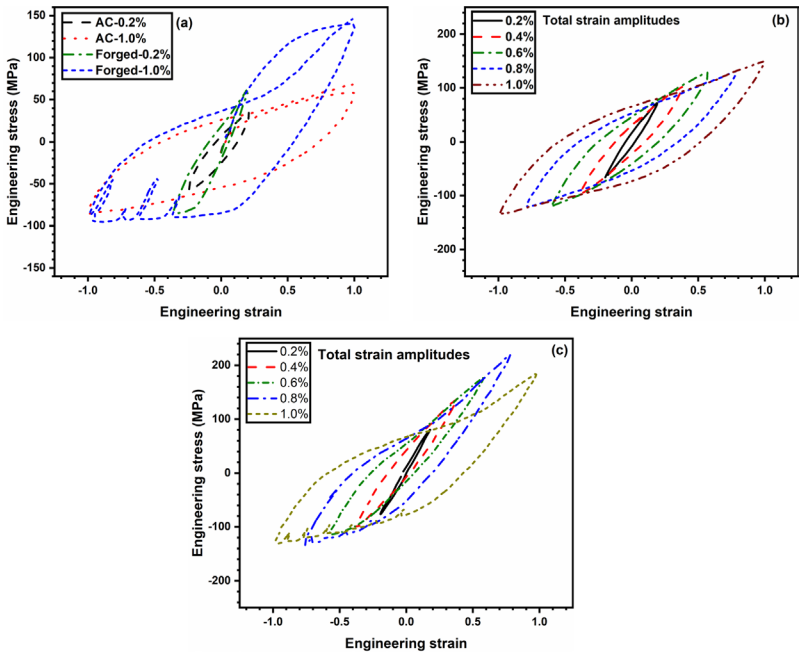

Fig. 8 *Stress vs. strain hysteresis loops are depicted for two conditions: (a) the initial cycle of both cast and forged materials; and (b, c) the half-life cycles for; (b) as-cast; and (c) forged AZ31B [94]*

3. Fatigue Crack Growth Modelling

3.1 Constant Amplitude Loading (CAL)

The experimental data attained from the FCG results of Mg alloy could be utilized to assess various pre-existing crack growth models. It was revealed [95–97] that the modification of Walker's model [98] by Kujawski [98,99] effectively acquired the impact of R-ratio on FCG. Wheeler's model [100] exhibited a reasonable capacity in predicting the overload effect and loading sequence effect [95–97]. These two models will be reconsidered to assess their effectiveness in modeling FCG of the Mg alloy. The mathematical representation of Walker's model [98] takes the following form,

$$\overline{K} = K_{max}^{\alpha} \Delta K^{(1-\alpha)} \tag{1}$$

where, $\overline{K}$: effective stress intensity factor (SIF), K_{max}: max. SIF, ΔK: SIF range and α: material constant. Kujawski [98,99] utilized a comparable effective SIF as Walker's approach.

$$k = K_{max}^{\alpha} (\Delta K^{+})^{(1-\alpha)} \tag{2}$$

where, ΔK^{+}: positive portion of the SIF range, and *k*: effective SIF.

3.2 Overload and Sequence Loading

In order to enable estimates of OL and sequence load impacts, it is necessary to mathematically characterize the experimental FCG results under CAL. The Paris power law eq. [101] is employed to depict the correlation between the FCG rate (da/dN) and the effective SIF (*k*).

$$da/dN = Ck^{n} \tag{3}$$

where, *C* and *n* are material constant. For representing the impact of OL, underloading (UL), and sequential loading, Wheeler [91,100] introduced a model that can be formulated through the subsequent eq. after the following change.

$$da/dN = \emptyset_R Ck^{n} \tag{4}$$

where, $\emptyset_R$: retardation factor. The formulation of the retardation correction factor is presented as follows,

$$\emptyset_R = \begin{cases} \left[\frac{r_{pi}}{a_{OL}+r_{p,OL}-a_i}\right]^m, & a_i + r_{pi} \le a_{OL} + r_{p,OL} \\ 1, & a_i + r_{pi} \ge a_{OL} + r_{p,OL} \end{cases} \quad (5)$$

where, r_{pi}: current cyclic plastic zone size at ith cycle, a_{OL}: crack length at which the OL is applied, $r_{p,OL}$: the plastic zone size after the OL, a_i: current crack length at ith cycle, and m: variable shaping constant. Irwin's technique can be employed for calculating the size of the cyclic plastic zone under conditions of plane stress [102].

$$r_{pi} = \frac{1}{4\pi}\left(\frac{\Delta K_i}{\sigma_y}\right)^2 \quad (6)$$

where, ΔK_i: SIF range at ith loading cycle, σ_y: tensile yield stress. The calculation of the plastic zone size arising from a monotonic overload is achieved through the following equation [102].

$$r_{p,OL} = \frac{1}{\pi}\left(\frac{K_{OL}}{\sigma_y}\right)^2 \quad (7)$$

where, K_{OL}: SIF corresponding to the OL. Salvati et al. [91] reported that the Walker-Wheeler model are visually depicted on the Paris equivalent SIF $\Delta K_{eq.}$ versus FCG rate (da/dN) as illustrated in Fig. 9(a & b). Employing the model resulted in a satisfactory agreement with the experimental data. Fig. 9 clearly exhibits a strong level of agreement, distinguished by minimal dispersion and variance. This observation is of significance since the Wheeler model is formulated upon the correlation between the plastic radius and the magnitude of the overload effect.

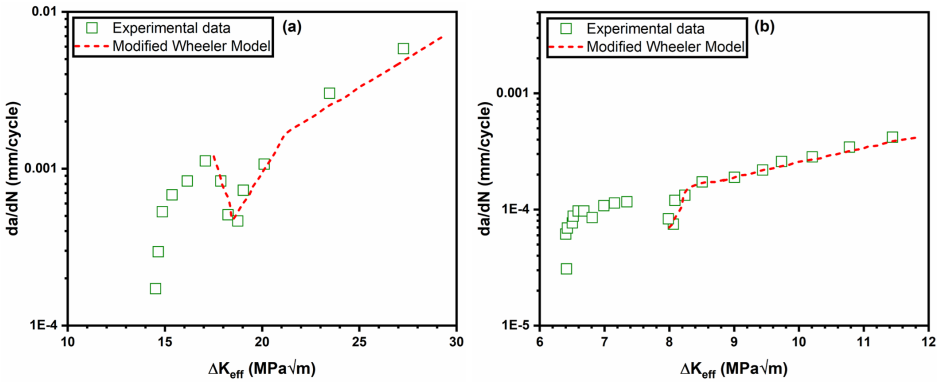

Fig. 9 *Modeled and experimental FCG rates for the following loading conditions: (a) R=0.1; (b) R=0.7 [91]*

4. Finite Element Modelling

Nonlinear finite-element analysis and modern computational tools built in commercial FE-based software packages have been beneficial to modern-day engineers and physicists. Nonlinear finite element analysis can also solve any intricate static or dynamic problem and model any kinematic and material nonlinearities present in the structure. The chosen element type, material model, failure criteria, and contact may reflect the accuracy and efficiency of the results shown in Table 7. The validation of the numerical model with experimental outcomes demonstrates the accuracy and dependability of the nonlinear finite element results. Xie et al. [103] reported that the contours of elastic strain components (EE_{11}, EE_{22}, and EE_{12}) in proximity to the crack tip at K_{max}. These plots pertain to three distinct cases, each featuring a crack length of 9 *mm*, all under the condition of plane-stress. The position of the crack tip is identified once the crack opening displacement (COD) reaches the value of δ_n. The graphical representation of the relationship between crack extension (Δa) and the number of cycles (N) is depicted in Fig. 10 for the three aforementioned scenarios, as deduced from simulation [103].

5. Effect of Twining and Detwinning

Metals possessing a crystal structure of body-centred cubic (BCC) and hexagonal close-packed (HCP) are more likely to undergo mechanical twinning at low temperatures and high strain rates. This is because the required flow stress for twin formation can be achieved in these types of metals [109]. Reversible twinning and detwinning were observed during the baseline tensile loading and unloading, specifically at a distance of 0.5 mm from the crack tip. This indicates that the volume which underwent twinning during the tensile loading phase was entirely detwinned during unloading [4]. If the stress and strain are sufficiently high at a given reversal

Int. Journal of Integrated Engineering Vol. 16 No. 6 (2024) p. 265-284

point, the stress-strain hysteresis loop can display a clear plateau during fatigue and deformation twinning [16]. Because of the HCP structure, twinning is crucial to how plasticity develops in magnesium alloys. The previously described basal and non-basal slip structures only provide four distinct deformation processes. Therefore, it is observed that the optimal locations for crack nucleation are low-energy coherent twin boundaries [110]. The activation stress for basal slip (in tension) or extension twinning (in compression) is relatively low at ambient temperature. Under cyclic loading, the actions of twinning and detwinning would take on a significant amount of the cyclic strain [111].

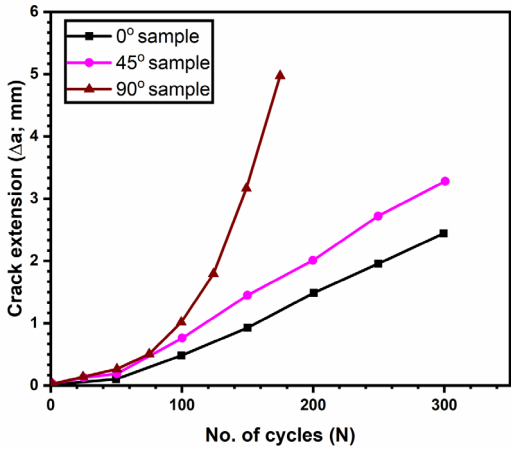

Fig. 10 *The correlation between crack extension (Δa) and No. of cycles (N) at different orientations [103]*

Table 7 *FEM simulation of Mg alloys*

Author	Software used	Loading	Material used	Material model	Element type	Mesh size
Yu et al. 2017 [11]	Abaqus/CAE 6.11-PR3	Semi-cylindrical loading	AZ31B	-	8-node linear elements	50 μm and 50μm 98,576 nodes and 89,760 elements
Liu et al. 2012 [28]	ANSYS 13.0	Tensile Impact Bending	AZ31B Al 6063	-	-	-
Kim et al. 2008 [61]	FEM simulation code MARC	Fatigue	AZ31	Large displacement, contact, and elastic-plastic behavior.		4-node 3D quadrilateral shell elements
Jiang et al. 2009 [104]	ABAQUS MSC.Fatigue	Fatigue	ZK60	Isotropic and the plastic strain	C3D8R element	-
Salvati et al. 2016 [91]	FEM Software	Fatigue	AZ31B	Elastoplastic regime	8-node linear brick elements	Mesh size is 0.02mm and 0.02mm. 27 000 elements
Jiang et al. 2012 [105]	ABAQUS MSC.Fatigue	Fatigue Tensile	AZ31B and ZK60	-	-	-
Chandola et al. 2015 [106]	ABAQUS	Fatigue	AZ31	Anisotropic elastic–plastic model	C3D8R	1290 hexahedral elements

Orhorhoro et al. 2018 [107]	ANSYS 16.0	Fatigue	AM50	-	-	Element size is 3 mm
Isahak et al. 2021 [108]	ABAQUS	Tensile Fatigue	AZ31B HSS SMP	-	-	The Mesh element size is 1.0 mm and the tolerance value is 0.05 mm.

The main reason why twinning and precipitation interact is that it is hard to move the boundaries of twins when there are a lot of precipitations. Fig. 11 shows a simplified picture of a precipitate or particle blocking twinning to better understand how a twin and a plate-shaped precipitate interact [112]. The fatigue life is not directly affected by the deformation twining of {1 0 $\bar{1}$ 2} type as it was found below and beyond the fatigue limit [113]. Deformation twinning is favored in coarse-grain magnesium alloys under in-plane compression, especially in basal-textured magnesium sheets, leading to lower yield stress compared to in-plane tension [80]. Transgranular cracking is the most common form of FCP in all three specimen orientations. Transgranular cracking is mostly caused by slip-induced cleavage in T-L and L-T samples. In T-R samples, twin boundary cracking and slip-induced cleavage can be seen [5]. A slip-to-fracture-influenced surface is formed when the detwinning stops if the crack and plastic zone size increases at the crack tip. Fig. 12 shows in a simplified way how the typical AZ31 fatigue fracture morphology is formed [114].

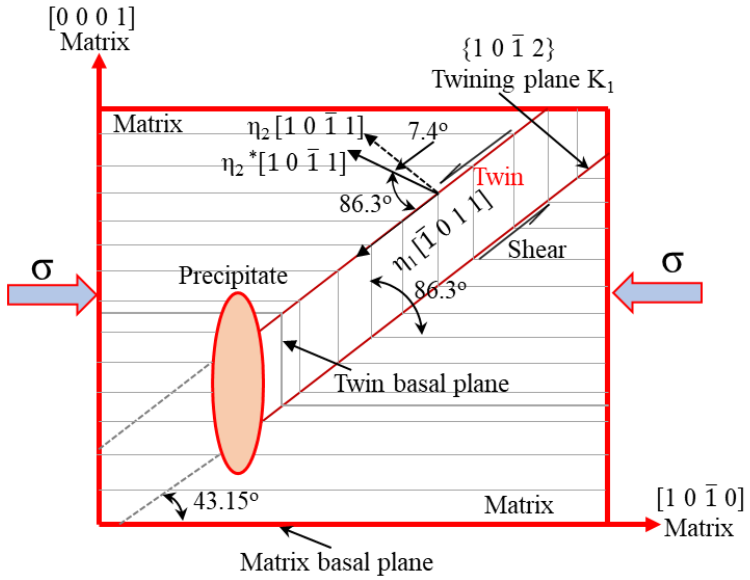

Fig. 11 *The diagram depicts the interplay between a plate-shaped precipitate and a {1 0 $\bar{1}$ 2 } twin in the GW103K [112]*

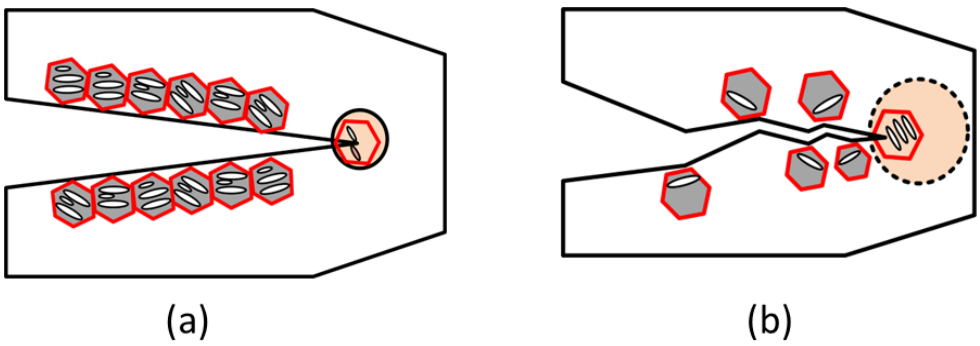

Fig. 12 *(a and b) Diagram illustrating how the usual fatigue fracture morphologies of magnesium alloys are formed [114]*

6. Conclusion and Future Scope

The experimental work and numerical analysis on several magnesium alloys are reviewed in this study. The comparison and discussion of monotonic tensile, compressive, and cyclic behaviour under various loading conditions are also given. The behavior of magnesium alloy under varying conditions is elucidated through a comprehensive examination. Firstly, the rate of stress softening in the alloy is found to escalate with increasing applied strain amplitudes, particularly evident in samples subjected to larger strain amplitudes during initial and final loading cycles. At ambient temperature, the alloy's elongation at fracture diminishes as the strain rate increases, although within the temperature range of 373K to 523K, the AZ31B Mg alloy displays heightened elongation with higher strain rates. Additionally, at elevated temperatures, the alloy exhibits reduced flow stress alongside a notable increase in elongation at fracture under high strain rate conditions. The material demonstrates positive strain rate sensitivity at RT, with this sensitivity escalating with rising temperatures while decreasing strain rates enhance the material's temperature sensitivity. Furthermore, at high temperatures, plastic strain amplitude increases while material strength decreases, albeit twinning phenomena occur less prominently compared to lower temperatures, initiating at higher stress levels and delaying onset. Elevating the temperature to 473K results in a significant reduction in mean stresses under cyclic loading, indicating a more symmetrical behavior, while decreasing loading frequency correlates with increased fatigue crack propagation rate. Lastly, the evaluation of fatigue life models using experimental data highlights the efficacy of the energy-based Jahed-Varvani (JV) model in predicting magnesium alloy fatigue life across a spectrum of temperatures.

- A substantial study is required to identify FCG behavior and fatigue life prediction approaches for magnesium alloys under various load ratios and overload ratios at elevated temperatures. The information provided below are intended to be beneficial for future research:
- The investigation and understanding of fatigue crack growth phenomena remain inadequate, particularly concerning elevated temperatures and subzero temperature conditions within the scientific literature. The behaviour of AZ31B alloys has not been studies for low cycle fatigue at subzero temperatures.
- There are few studies on the impact of temperature and pre-strain on the high cycle fatigue behavior of Mg alloy AZ31B.
- Within the realm of, there exists a paucity of comprehensive studies for magnesium alloy AZ31B delving into the intricate interplay between temperature variations and pre-strain effects on its high cycle fatigue behavior. The current scientific literature reveals a conspicuous gap in understanding the nuanced responses of this alloy to varying thermal environments and pre-strain conditions, particularly within the context of high cycle fatigue analysis.
- The residual mechanical properties of the AZ31B alloy post-fire exposure remain largely unexplored in scientific literature. Understanding its response to extreme thermal conditions is crucial, yet research in this area is scarce. Investigating the post-fire mechanical behavior of AZ31B is essential for assessing its performance and durability in fire-related scenarios.

Acknowledgement

The authors would like to thank the Department of Mechanical Engineering, National Institute of Technology Srinagar, Jammu and Kashmir (India) for supporting this work.

Conflict of Interest

Authors declare that there is no conflict of interests regarding the publication of the paper.

Author Contribution

The authors confirm contribution to the paper as follows: ***study conception and design:*** *Raj Kumar, G. A. Harmain;* ***data collection:*** *Raj Kumar, Mohammad Mursaleen;* ***analysis and interpretation of results:*** *Raj Kumar, Mohammad Mursaleen, G. A. Harmain;* ***draft manuscript preparation:*** *Raj Kumar, Mohammad Mursaleen, G. A. Harmain; All authors reviewed the results and approved the final version of the manuscript*

References

[1] Agnew, S. R. (2005). Plastic anisotropy and the role of non-basal slip in magnesium alloy AZ31B. *International Journal of Plasticity*, *21*, 1161–1193. https://doi.org/10.1016/j.ijplas.2004.05.018

[2] Albinmousa, J., Jahed, H., & Lambert, S. (2011a). Cyclic axial and cyclic torsional behaviour of extruded AZ31B magnesium alloy. *International Journal of Fatigue*, *33*(11), 1403–1416. https://doi.org/10.1016/j.ijfatigue.2011.04.012

[3] Albinmousa, J., Jahed, H., & Lambert, S. (2011b). Cyclic behaviour of wrought magnesium alloy under multiaxial load. *International Journal of Fatigue*, *33*(8), 1127–1139. https://doi.org/10.1016/j.ijfatigue.2011.01.009

[4] Albinmousa, J., Peron, M., Jose, J., Abdelaal, A. F., & Berto, F. (2020). Fatigue of V-notched ZK60 magnesium samples: X-ray damage evolution characterization and failure prediction. *International Journal of Fatigue*, *139*(March). https://doi.org/10.1016/j.ijfatigue.2020.105734

[5] Anes, V., Lage, Y. E., Vieira, M., Maia, N. M. M., Freitas, M., & Reis, L. (2016). Torsional and axial damping properties of the AZ31B-F magnesium alloy. *Mechanical Systems and Signal Processing*, 1–11. https://doi.org/10.1016/j.ymssp.2016.02.040

[6] Anes, V., Reis, L., & Freitas, M. (2021). Fatigue damage map of az31b-f magnesium alloys under multiaxial loading conditions. *Metals*, *11*(10), 1–17. https://doi.org/10.3390/met11101616

[7] Begum, S., Chen, D. L., Xu, S., & Luo, A. A. (2009a). *Effect of strain ratio and strain rate on low cycle fatigue behavior of AZ31 wrought magnesium alloy*. *517*, 334–343. https://doi.org/10.1016/j.msea.2009.04.051

[8] Begum, S., Chen, D. L., Xu, S., & Luo, A. A. (2009b). Low cycle fatigue properties of an extruded AZ31 magnesium alloy. *International Journal of Fatigue*, *31*(4), 726–735. https://doi.org/10.1016/j.ijfatigue.2008.03.009

[9] Bhaumik, S. K., Sujata, M., & Venkataswamy, M. A. (2008). *Fatigue failure of aircraft components*. *15*, 675–694. https://doi.org/10.1016/j.engfailanal.2007.10.001

[10 Bohlen, J., Nu, M. R., Senn, J. W., Letzig, D., & Agnew, S. R. (2007). *The texture and anisotropy of magnesium – zinc – rare earth alloy sheets*. *55*, 2101–2112. https://doi.org/10.1016/j.actamat.2006.11.013

[11] Cauthen, C., Daniewicz, S. R., & Shamsaei, N. (2017). Modeling fatigue crack growth behavior in rolled AZ31 magnesium alloy using CTOD based strip yield modeling. *International Journal of Fatigue*, *96*, 196–207. https://doi.org/10.1016/j.ijfatigue.2016.11.031

[12] Chandola, N., Lebensohn, R. A., Cazacu, O., Revil-baudard, B., Mishra, R. K., & Barlat, F. (2015). International Journal of Solids and Structures Combined effects of anisotropy and tension – compression asymmetry on the torsional response of AZ31 Mg. *International Journal of Solids and Structures*, *58*, 190–200. https://doi.org/10.1016/j.ijsolstr.2015.01.001

[13] Chen et al. (2015). Ratcheting and low-cycle fatigue characterizations of extruded AZ31B Mg alloy with and without corrosive environment. *International Journal of Fatigue*, *80*, 364–371. https://doi.org/10.1016/j.ijfatigue.2015.06.022

[14] Chen, L., Wang, C., Wu, W. E. I., Liu, Z., Stoica, G. M., Wu, L., & Liaw, P. K. (2007). *Low-Cycle Fatigue Behavior of an As-Extruded AM50 Magnesium Alloy*. *38*(September), 2235–2241. https://doi.org/10.1007/s11661-007-9181-y

[15] Choi, S. S. (2018). Characteristics of Empirical Cumulative Distribution Function of Grown Crack Size under Different Maximum Fatigue Loads in AZ31. *IOSR Journal of Engineering (IOSRJEN)*, *08*(01), 40–45.

[16] Choi, S. S. (2020). Evaluating the Effect of Specimen Thickness on Fatigue Crack Growth in AZ31 Alloy Using ANOVA. *The Korean Society of Manufacturing Process Engineers*, *19*(6), 9–16. https://doi.org/10.14775/ksmpe.2020.19.06.009

[17] Cui et al. (2015). *Research on fatigue crack growth behavior of AZ31B magnesium alloy electron beam welded joints based on temperature distribution around the crack tip*. *133*(79), 14–23. https://doi.org/10.1016/j.engfracmech.2014.11.004

[18] Culbertson, D., & Jiang, Y. (2016). An experimental study of the orientation effect on fatigue crack propagation in rolled AZ31B magnesium alloy. *Materials Science and Engineering A*, *676*, 10–19. https://doi.org/10.1016/j.msea.2016.08.088

[19] Daneshpour, S., Koçak, M., Langlade, S., & Horstmann, M. (2009). Effect of overload on fatigue crack retardation of aerospace Al-alloy laser welds using crack-tip plasticity analysis. *International Journal of Fatigue*, *31*(10), 1603–1612. https://doi.org/10.1016/j.ijfatigue.2009.04.005

[20] Daniel Kujawski. (2001). A new (_K+ Kmax) 0.5 driving force parameter for crack growth in aluminum alloys. *International Journal of Fatigue*, *23*, 733–740.

[21] Doege, E., & Dro, K. (2001). *Sheet metal forming of magnesium wrought alloys- formability and process technology*. *115*(1), 14–19. https://doi.org/https://doi.org/10.1016/S0924-0136(01)00760-9

[22] Eisenmeier, G., Holzwarth, B., Höppel, H. W., & Mughrabi, H. (2001). Cyclic deformation and fatique behaviour of the magnesium alloy AZ91. *Materials Science and Engineering A*, *319–321*, 578–582. https://doi.org/10.1016/S0921-5093(01)01105-4

[23] Feng et al. (2014). Experimental study on tensile property of AZ31B magnesium alloy at different high strain rates and temperatures. *JOURNAL OF MATERIALS&DESIGN*, *57*, 10–20. https://doi.org/10.1016/j.matdes.2013.12.031

[24] Ge, M. Z., & Xiang, J. Y. (2016). Effect of laser shock peening on microstructure and fatigue crack growth rate of AZ31B magnesium alloy. *Journal of Alloys and Compounds*, *680*, 544–552. https://doi.org/10.1016/j.jallcom.2016.04.179

[25] Ghorbanpour, S., Mcwilliams, B. A., & Knezevic, M. (n.d.). *Low-cycle fatigue behavior of rolled WE43-T5 magnesium alloy*. 0–1. https://doi.org/10.1111/ffe.12992
[26] Gryguć, A., Behravesh, S. B., Shaha, S. K., Jahed, H., Wells, M., Williams, B., & Su, X. (2019). Multiaxial cyclic behaviour of extruded and forged AZ80 Mg alloy. *International Journal of Fatigue*, *127*(June), 324–337. https://doi.org/10.1016/j.ijfatigue.2019.06.015
[27] Guo, X., Lanc, D., Yang, W., & Brnic, J. (2014). *Low cycle fatigue and mechanical properties of magnesium alloy Mg – 6Zn – 1Y – 0 . 6Ce – 0 . 6Zr at different temperatures*. *59*, 287–295. https://doi.org/10.1016/j.matdes.2014.03.001
[28] Gwynne, B., & Lyon, P. (2007). Magnesium alloys in aerospace applications, past concerns, current solutions. *Triennial International Aircraft Fire & Cabin Safety Research Conference*.
[29] Han et al. (2014). Acoustic emission study of fatigue crack propagation in extruded AZ31 magnesium alloy. *Materials Science and Engineering A*, *597*, 270–278. https://doi.org/10.1016/j.msea.2013.12.083
[30[Hasegawa, S., Tsuchida, Y., Yano, H., & Matsui, M. (2007). *International Journalof Fatigue Evaluation of low cycle fatigue life in AZ31 magnesium alloy*. *29*, 1839–1845. https://doi.org/10.1016/j.ijfatigue.2006.12.003
[31] He, C., Liu, Y., Li, J., Yang, K., Wang, Q., & Chen, Q. (2017). *Very-high-cycle fatigue crack initiation and propagation behaviours of magnesium alloy ZK60*. *0836*(December). https://doi.org/10.1080/02670836.2017.1407556
[32] Hongxia et al. (2011). As-extruded AZ31B Magnesium Alloy Fatigue Crack Propagation Behavior. *Journal of Wuhan University of Technology-Mater. Sci. Ed*, *26*(6), 1114–1120. https://doi.org/10.1007/s11595-011-0373-3
[33] Hongxia et al. (2012). Fatigue Crack Propagation Behavior of as-Extruded AZ31B Mg Alloy Welded Joint. *Rare Metal Materials and Engineering*, *41*(6), 967–972. https://doi.org/10.1016/S1875-5372(12)60054-X
[34] Horstemeyer, M. F., Yang, N., Gall, K., Mcdowell, D. L., Fan, J., & Gullett, P. M. (2004). *High cycle fatigue of a die cast AZ91E-T4 magnesium alloy*. *52*, 1327–1336. https://doi.org/10.1016/j.actamat.2003.11.018
[35] Hyuk, S., Hong, S., Bang, W., & Soo, C. (2010). *Effect of anisotropy on the low-cycle fatigue behavior of rolled AZ31 magnesium alloy*. *527*, 417–423. https://doi.org/10.1016/j.msea.2009.08.044
[36] Hyuk, S., Hong, S., Ho, B., Bang, W., & Soo, C. (2010). Low-cycle fatigue characteristics of rolled Mg – 3Al – 1Zn alloy. *International Journal of Fatigue*, *32*(11), 1835–1842. https://doi.org/10.1016/j.ijfatigue.2010.05.002
[37] Isahak, A. H., Abdullah, M. F., Faidzi, M. K., Yusoff, W. Y. W., Abdullah, S., Ali, A., & Mubasyir, M. M. (2021a). A Study of Stress Behaviour and Energy Absorption for Sandwich Metal Panel Compared to Solid Material under Static Condition. *Journal of Failure Analysis and Prevention*, *21*(6), 2021–2028. https://doi.org/10.1007/s11668-021-01278-5
[38] Isahak, A. H., Abdullah, M. F., Faidzi, M. K., Yusoff, W. Y. W., Abdullah, S., Ali, A., & Mubasyir, M. M. (2021b). A Study of Stress Behaviour and Energy Absorption for Sandwich Metal Panel Compared to Solid Material under Static Condition. *Journal of Failure Analysis and Prevention*. https://doi.org/10.1007/s11668-021-01278-5
[39] Ishihara et al. (2009). The effect of load ratio on fatigue life and crack propagation behavior of an extruded magnesium alloy. *International Journal of Fatigue*, *31*(11–12), 1788–1794. https://doi.org/10.1016/j.ijfatigue.2009.02.034
[40] Ishihara, S., Nan, Z., & Goshima, T. (2007). *Effect of microstructure on fatigue behavior of AZ31 magnesium alloy*. *470*(May 2006), 214–222. https://doi.org/10.1016/j.msea.2006.09.124
[41] Jabbari et al. (2020). Low cycle fatigue behavior of AZ31B extrusion at elevated temperatures. *International Journal of Fatigue*, *139*(March), 105803. https://doi.org/10.1016/j.ijfatigue.2020.105803
[42] Jahed, H., & Albinmousa, J. (2014). Multiaxial behaviour of wrought magnesium alloys – A review and suitability of energy-based fatigue life model. *Theoretical and Applied Fracture Mechanics*, *73*, 97–108. https://doi.org/10.1016/j.tafmec.2014.08.004
[43] Jain, J., Poole, W. J., Sinclair, C. W., & Gharghouri, M. A. (2010). Reducing the tension – compression yield asymmetry in a Mg – 8Al – 0 . 5Zn alloy via precipitation. *Scripta Materialia*, *62*(5), 301–304. https://doi.org/10.1016/j.scriptamat.2009.11.024
[44] Jiang, L. (2007). Twinning and texture development in two Mg alloys subjected to loading along three different strain paths. *Acta Materialia*, *55*(11), 3899–3910. https://doi.org/10.1016/j.actamat.2007.03.006
[45] Jiang, L., Jonas, J. J., Luo, A. A., & Sachdev, A. K. (2006). *Twinning-induced softening in polycrystalline AM30 Mg alloy at moderate temperatures*. *54*, 771–775. https://doi.org/10.1016/j.scriptamat.2005.11.029
[46] Jiang, S. Q., Zhou, J. Z., Fan, Y. J., Huang, S., & Zhao, J. F. (2009). *Prediction on Residual Stress and Fatigue Life of Magnesium Alloy Treated by Laser Shot Peening*. *627*, 393–398. https://doi.org/10.4028/www.scientific.net/MSF.626-627.393
[47] Jiang, S., & Xu, H. (2012). *Numerical Study on Strengthening Effect of Laser Shot Peening for Wrought*

Magnesium Alloy. *219*, 2234–2237. https://doi.org/10.4028/www.scientific.net/AMM.217-219.2234
[48] Junak, G. (2020). *Fatigue Properties of AZ31 and WE43 Magnesium Alloys*. *65*, 721–726. https://doi.org/10.24425/amm.2020.132811
[49] Khan, A. A., & Marrow, T. J. (2009). In-situ observation of damage mechanisms by digital image correlation during tension and low cycle fatigue of magnesium alloys. *12th International Conference on Fracture 2009, ICF-12*, *2*(July 2009), 871–879.
[50] Khan et al. (2011). Mechanical response and texture evolution of AZ31 alloy at large strains for different strain rates and temperatures. *International Journal of Plasticity*, *27*(5), 688–706. https://doi.org/10.1016/j.ijplas.2010.08.009
[51] Kim, W. J., Kim, H. K., Kim, W. Y., & Han, S. W. (2008). *Temperature and strain rate effect incorporated failure criteria for sheet forming of magnesium alloys*. *488*, 468–474. https://doi.org/10.1016/j.msea.2007.11.077
[52] Koike, J., Fujiyama, N., Ando, D., & Sutou, Y. (2010). Roles of deformation twinning and dislocation slip in the fatigue failure mechanism of AZ31 Mg alloys. *Scripta Materialia*, *63*(7), 747–750. https://doi.org/10.1016/j.scriptamat.2010.03.021
[53] Kulekci, M. K. (2015). *Magnesium and its alloys applications in automotive industry*. *2008*, 851–865. https://doi.org/10.1007/s00170-007-1279-2
[54] Kumar, R., Mursaleen, M., Harmain, G. A., & Kumar, A. (2023). A Critical Review of Fatigue Life Prediction on 316LN SS. *Advances in Modelling and Optimization of Manufacturing and Industrial Systems*, 427–440. https://doi.org/https://doi.org/10.1007/978-981-19-6107-6_30
[55] Lei, Y., Li, H., Liu, Y., Wang, Z., & Kang, G. (2023). Experimental study on uniaxial ratchetting-fatigue interaction of extruded AZ31 magnesium alloy with different plastic deformation mechanisms. *Journal of Magnesium and Alloys*, *11*(1), 379–391. https://doi.org/10.1016/j.jma.2021.03.018
[56] Li, Q. (2021). Fatigue behavior of fine-grained magnesium under tension-tension loading at 0 ◦ C. *International Journal of Fatigue*, *153*(June), 106506. https://doi.org/10.1016/j.ijfatigue.2021.106506
[57] Liu, J., Zhao, Y., Song, L., & Xiang, Z. (2012). *Study on the AZ31B magnesium alloy in the application on high-speed trains*. *537*, 875–879. https://doi.org/10.4028/www.scientific.net/AMR.535-537.875
[58] Lu, Y., Taheri, F., & Gharghouri, M. (2008). *Study of fatigue crack incubation and propagation mechanisms in a HPDC AM60B magnesium alloy*. *466*, 214–227. https://doi.org/10.1016/j.jallcom.2007.11.115
[59] Luo, T. J., Yang, Y. S., Tong, W. H., Duan, Q. Q., & Dong, X. G. (2010). Fatigue deformation characteristic of as-extruded AM30 magnesium alloy. *Materials and Design*, *31*(3), 1617–1621. https://doi.org/10.1016/j.matdes.2009.08.042
[60] Mao, P., Liu, Z., Wang, C., Guo, Q., Sun, J., Wang, F., & Lin, L. (2008). Fatigue behavior of magnesium alloy and application in auto steering wheel frame. *Transactions of Nonferrous Metals Society of China*, *18*, s218–s222. https://doi.org/10.1016/S1003-6326(10)60206-3
[61] Meyers, M. A., Vöhringer, O., & Lubarda, V. A. (2001). The onset of twinning in metals: A constitutive description. *Acta Materialia*, *49*(19), 4025–4039. https://doi.org/10.1016/S1359-6454(01)00300-7
[62] Mirza, F. A., Chen, D. L., Li, D. J., & Zeng, X. Q. (2013). *Effect of rare earth elements on deformation behavior of an extruded Mg – 10Gd – 3Y – 0 . 5Zr alloy during compression*. *46*, 411–418. https://doi.org/10.1016/j.matdes.2012.10.040
[63] Mirza, F. A., Chen, D. L., Li, D. J., & Zeng, X. Q. (2014a). *Low cycle fatigue of a rare-earth containing extruded magnesium alloy Materials Science & Engineering A*. *June*. https://doi.org/10.1016/j.msea.2013.03.041
[64] Mirza, F. A., Chen, D. L., Li, D. J., & Zeng, X. Q. (2014b). *Low cycle fatigue of an extruded Mg – 3Nd – 0 . 2Zn – 0 . 5Zr magnesium alloy*. *64*, 63–73. https://doi.org/10.1016/j.matdes.2014.07.016
[65] Mokhtarishirazabad, M., Azadi, M., Hossein, G., Winter, G., & Eichlseder, W. (2013). Materials Science & Engineering A Improvement of high temperature fatigue lifetime in AZ91 magnesium alloy by heat treatment. *Materials Science & Engineering A*, *588*, 357–365. https://doi.org/10.1016/j.msea.2013.09.067
[66] Morita, S., Matsushita, K., Mayama, T., Hirai, T., Enjoji, T., & Hattori, N. (2011). *Fatigue-Fractured Surfaces and Crack Paths of Textured Polycrystalline Magnesium Alloys*. 571–578.
[67] Nan, Z. Y., Ishihara, S., Mcevily, A. J., Shibata, H., & Komano, K. (2007). *On the sharp bend of the S – N curve and the crack propagation behavior of extruded magnesium alloy*. *56*, 649–652. https://doi.org/10.1016/j.scriptamat.2007.01.009
[68] Nascimento, L., Yi, S., Bohlen, J., Fuskova, L., Letzig, D., & Kainer, K. U. (2010). Procedia Engineering High Cycle Fatigue Behaviour of Magnesium Alloys. *Procedia Engineering*, *2*(1), 743–750. https://doi.org/10.1016/j.proeng.2010.03.080
[69] Ni, D. R., Chen, D. L., Yang, J., & Ma, Z. Y. (2014). Low cycle fatigue properties of friction stir welded joints of a semi-solid processed AZ91D magnesium alloy. *Materials and Design*, *56*, 1–8. https://doi.org/10.1016/j.matdes.2013.10.081
[70] Noster, U., Altenberger, I., & Scholtes, B. (2006). Isothermal Fatigue of Magnesium Wrought Alloy AZ31. In *Magnesium Alloys and their Applications* (pp. 312–317). https://doi.org/10.1002/3527607552.ch49

[71] Noster, U., & Scholtes, B. (2003). Isothermal strain-controlled quasi-static and cyclic deformation behavior of magnesium wrought alloy AZ31. *Zeitschrift Fuer Metallkunde/Materials Research and Advanced Techniques*, *94*(5), 559–563. https://doi.org/10.3139/146.030559

[72] Orhorhoro, E. K., Essienubong, I. A., & Joel, O. O. (2018). Failure Analysis and Optimization of Aircraft Wheel Hub for Optimum Landing Scenario. *International Journal of Engineering Trends and Technology*, *60*(2), 135–141. https://doi.org/10.14445/22315381/ijett-v60p219

[73] Park, S. S., Tang, W. N., & You, B. S. (2010). Microstructure and mechanical properties of an indirect-extruded Mg – 8Sn – 1Al – 1Zn alloy. *Materials Letters*, *64*(1), 31–34. https://doi.org/10.1016/j.matlet.2009.09.062

[74] Pascu, A. M., Luo, A., & Zhang, L. (2010). Monotonic and Fatigue Behavior of Magnesium Extrusion Alloy AM30 : An International Benchmark Test in the " Magnesium Front End Research and Development Project " Institute of Metal Research Chinese Academy of Sciences. *SAE Technical Paper*, *April*, 0407. https://doi.org/10.4271/2010-01-0407

[75] Pirondi, A., Nicoletto, G., & Cn, R. K. (2005). *Fatigue crack paths in coarse-grained magnesium*. 237–244. https://doi.org/10.1111/j.1460-2695.2004.00832.x

[76] Pook, L. P., & Greenan, A. F. (1973). Fatigue crack-growth characteristics of two magnesium alloys. *Engineering Fracture Mechanics*, *5*(4), 935–946. https://doi.org/10.1016/0013-7944(73)90058-1

[77] Pugno, N., Ciavarella, M., Cornetti, P., & Carpinteri, A. (2006). A generalized Paris' law for fatigue crack growth. *Journal of the Mechanics and Physics of Solids*, *54*(7), 1333–1349. https://doi.org/10.1016/j.jmps.2006.01.007

[78] Qiao, H., Xin, Y. C., Zong, Z. L., & Wu, P. D. (2021). *International Journal of Solids and Structures Effect of twinning on the yield surface shape of Mg alloy plates under in- plane biaxial loading*. *216*, 211–221. https://doi.org/10.1016/j.ijsolstr.2021.01.029

[79] Rodriguez et al. (2016). Effect of strain rate and temperature on fracture of magnesium alloy. *Acta Materialia*, *112*(2016), 194–208. https://doi.org/10.1016/j.actamat.2016.03.061

[80] Rozali, S., & Mutoh, Y. (2009). *Effect of Stress Ratio on Fatigue Crack Growth Behavior of Magnesium Alloy AZ61 under 3 . 5 Mass % NaCl Spray Environment *.* *3*(12), 1274–1284. https://doi.org/10.1299/jmmp.3.1274

[81] Salvati, B. E., Sui, T., Zhang, H., Lunt, A. J. G., Fong, K. S., Song, X., & Korsunsky, A. M. (2016). *Elucidating the Mechanism of Fatigue Crack Acceleration Following the Occurrence of an Underload*. 1–12. https://doi.org/10.1002/adem.201600069

[82] Shahbeigi, P., & Apu, R. (2015). *Fracture Behavior of AZ31 Magnesium Alloy During Low-Stress High-Temperature Deformation*. 91–101. https://doi.org/10.1007/s13632-015-0189-1

[83] Singh, N. K., Kumar, D., & Chandel, P. (2020). Dynamic tensile behaviour of magnesium alloy AZ41 at different strain rates and temperatures. *U.P.B. Sci. Bull., Series D*, *82*(1).

[84] Tada, H., Paris, P. C., & Irwin, G. R. (1973). The stress analysis of cracks. *Handbook, Del Research Corporation*, *34*(1973).

[85] Temperatures, E. (2014). *Mechanical Behavior of AZ31B Mg Alloy Sheets under Monotonic and Cyclic Loadings at Room and Moderately Elevated Temperatures*. 1271–1295. https://doi.org/10.3390/ma7021271

[86] Tokaji, K., Nakajima, M., & Uematsu, Y. (2009). Fatigue crack propagation and fracture mechanisms of wrought magnesium alloys in different environments. *International Journal of Fatigue*, *31*(7), 1137–1143. https://doi.org/10.1016/j.ijfatigue.2008.12.012

[87] Toscano, D., Shaha, S. K., Behravesh, B., Jahed, H., & Williams, B. (2017). Effect of forging on the low cycle fatigue behavior of cast AZ31B alloy. *Materials Science and Engineering: A*, *706*(May), 342–356. https://doi.org/10.1016/j.msea.2017.08.086

[88] Uematsu, Y., Tokaji, K., & Matsumoto, M. (2009). *Effect of aging treatment on fatigue behaviour in extruded AZ61 and AZ80 magnesium alloys*. *517*, 138–145. https://doi.org/10.1016/j.msea.2009.03.066

[89] Walker, K. (1970). *The effect of stress ratio during crack propagation and fatigue for 2024-T3 and 7075-T6 aluminum*.

[90] Wang, X., Gao, Z., Zhao, T., & Jiang, Y. (2016). *An Experimental Study of the Crack Growth Behavior of 16MnR Pressure Vessel Steel*. *131*(April 2009), 1–9. https://doi.org/10.1115/1.3008034

[91] Wheatley, G., Hu, X. Z., & Estrin, Y. (1999). Effects of a single tensile overload on fatigue crack growth in a 316L steel. *Fatigue and Fracture of Engineering Materials and Structures*, *22*(12), 1041–1051. https://doi.org/10.1046/j.1460-2695.1999.00225.x

[92] Wheeler, O. E. (1972). Spectrum loading and crack growth. *Journal of Fluids Engineering, Transactions of the ASME*, *94*(1), 181–186. https://doi.org/10.1115/1.3425362

[93] Wu et al. (2008). Twinning – detwinning behavior during the strain-controlled low-cycle fatigue testing of a wrought magnesium alloy , ZK60A. *Acta Materialia*, *56*, 688–695. https://doi.org/10.1016/j.actamat.2007.10.030

[94] Wu, L., Agnew, S. R., Ren, Y., Brown, D. W., Clausen, B., Stoica, G. M., Wenk, H. R., & Liaw, P. K. (2010). *The effects of texture and extension twinning on the low-cycle fatigue behavior of a rolled magnesium alloy , AZ31B*. *527*, 7057–7067. https://doi.org/10.1016/j.msea.2010.07.047
[95] Wu, W., Lee, S. Y., Paradowska, A. M., Gao, Y., & Liaw, P. K. (2012). Twinning-detwinning behavior during fatigue-crack propagation in a wrought magnesium alloy AZ31B. *Materials Science and Engineering A*, *556*, 278–286. https://doi.org/10.1016/j.msea.2012.06.088
[96] Xie, D., Zhang, W., Lyu, Z., Liaw, P. K., Tran, H., Chew, H. B., Wei, Y., Ren, Y., & Gao, Y. (2022). Plastic anisotropy and twin distributions near the fatigue crack tip of textured Mg alloys from in situ synchrotron X-ray diffraction measurements and multiscale mechanics modeling. *Journal of the Mechanics and Physics of Solids*, *165*(April), 104936. https://doi.org/10.1016/j.jmps.2022.104936
[97] Xiong, Y., Yu, Q., & Jiang, Y. (2012). Multiaxial fatigue of extruded AZ31B magnesium alloy. *Materials Science & Engineering A*, *546*, 119–128. https://doi.org/10.1016/j.msea.2012.03.039
[98] Xu, D., Tang, W., Liu, L., Xu, Y., & Han, E. (2007). *The Fatigue Crack Propagation (FCP) Behavior of the Forged Mg-Zn-Y-Zr Alloy*. *549*, 343–346. https://doi.org/10.4028/www.scientific.net/MSF.546-549.343
[99] Xu et al. (2009). Effects of Strain Rate and Temperature on Tensile Flow Behavior and Energy Absorption of Extruded Magnesium AM30 Alloy. *Journal of Materials Engineering and Performance*, *18*(November), 1091–1101. https://doi.org/10.1007/s11665-008-9332-3
[100] Yamada, R., Yoshihara, S., & Ito, Y. (2021). Fatigue properties of az31b magnesium alloy processed by equal-channel angular pressing. *Metals*, *11*(8), 1–9. https://doi.org/10.3390/met11081191
[101] Yan, S., Hainsworth, S. V, & Lawes, S. D. A. (2015). Temperature Dependence of Low Cycle Fatigue Behavior in AZ31 Magnesium Alloy. *Materials Today: Proceedings*, *2*, S243–S250. https://doi.org/10.1016/j.matpr.2015.05.034
[102] Yang, F., Yin, S. M., Li, S. X., & Zhang, Z. F. (2008). *Crack initiation mechanism of extruded AZ31 magnesium alloy in the very high cycle fatigue regime*. *491*, 131–136. https://doi.org/10.1016/j.msea.2008.02.003
[103] Yang, Q., & Ghosh, A. K. (2006). *Deformation behavior of ultrafine-grain (UFG) AZ31B Mg alloy at room temperature*. *54*, 5159–5170. https://doi.org/10.1016/j.actamat.2006.06.043
[104] Yin, S. M., Yang, F., Yang, X. M., Wu, S. D., Li, S. X., & Li, G. Y. (2008). *The role of twinning – detwinning on fatigue fracture morphology of Mg – 3 % Al – 1 % Zn alloy*. *494*, 397–400. https://doi.org/10.1016/j.msea.2008.04.056
[105] Yoo, M. H. (1981). Slip, twinning, and fracture in hexagonal close-packed metals. *Metallurgical Transactions A*, *12*(3), 409–418. https://doi.org/10.1007/BF02648537
[106] Yu et al. (2017). Improvement on dynamic fracture properties of magnesium alloy AZ31B through equal channel angular pressing. *Engineering Fracture Mechanics*, *181*, 87–100. https://doi.org/10.1016/j.engfracmech.2017.07.002
[107] Yu, Q., Zhang, J., Jiang, Y., & Li, Q. (2012). An experimental study on cyclic deformation and fatigue of extruded ZK60 magnesium alloy. *International Journal of Fatigue*, *36*(1), 47–58. https://doi.org/10.1016/j.ijfatigue.2011.08.016
[108] Zeng, R. C., Ke, W., & Han, E. H. (2009). Influence of load frequency and ageing heat treatment on fatigue crack propagation rate of as-extruded AZ61 alloy. *International Journal of Fatigue*, *31*(3), 463–467. https://doi.org/10.1016/j.ijfatigue.2008.07.005
[109] Zeng, R. C., Xu, Y. B., Ke, W., & Han, E. H. (2009). *Fatigue crack propagation behavior of an as-extruded magnesium alloy AZ80*. *509*, 1–7. https://doi.org/10.1016/j.msea.2009.01.013
[110] Zeng, R., Han, E., & Ke, W. (2012). A critical discussion on influence of loading frequency on fatigue crack propagation behavior for extruded Mg – Al – Zn alloys. *International Journal of Fatigue*, *36*(1), 40–46. https://doi.org/10.1016/j.ijfatigue.2011.09.001
[111] Zeng, R., Han, E., Ke, W., Dietzel, W., Ulrich, K., & Atrens, A. (2010). Influence of microstructure on tensile properties and fatigue crack growth in extruded magnesium alloy AM60. *International Journal of Fatigue*, *32*(2), 411–419. https://doi.org/10.1016/j.ijfatigue.2009.07.021
[112] Zhao, T., Zhang, J., & Jiang, Y. (2008). A study of fatigue crack growth of 7075-T651 aluminum alloy. *International Journal of Fatigue*, *30*, 1169–1180. https://doi.org/10.1016/j.ijfatigue.2007.09.006
[113] Zheng et al. (2013). Loading history effect on fatigue crack growth of extruded AZ31B magnesium alloy. *Engineering Fracture Mechanics*, *114*, 42–54. https://doi.org/10.1016/j.engfracmech.2013.10.012
[114] Zhou et al. (2016). Mechanical Behavior and Microstructural Analysis of Extruded AZ31B Magnesium Alloy Processed by Backward Extrusion. *Journal of Materials*